REVIEW

Check for updates

Recent advances in ruthenium-based electrocatalysts for the hydrogen evolution reaction

Seo-Yoon Bae, [ID] [a] Javeed Mahmood, [ID] [a] In-Yup Jeon [ID] [b] and Jong-Beom Baek [ID] *[a]

Exploration of electrocatalysts for clean and sustainable hydrogen generation from water splitting has received huge attention due to the depletion of fossil fuels and environmental pollution. Although platinum (Pt) is the most efficient catalyst for the hydrogen evolution reaction (HER), it has limitations for widespread applications due to its towering cost, scarcity and instability. Various catalysts such as precious/non-precious metal and metal-free catalysts have been developed for a viable HER process. Among them, ruthenium (Ru) based catalysts, which possess appropriate hydrogen bonding energy and reasonable price, have demonstrated strong potential as an alternative to Pt for the HER. In this review article, we summarize recently developed Ru-based electrocatalysts with superior HER performance, *i.e.*, Ru on carbon supports, Ru phosphide based catalysts, and Ru coupled with transition metals. Finally, we discuss the challenges and perspectives of Ru-based catalysts in the HER research field.

1. Introduction

Due to growing concerns about the approaching energy crisis and environmental pollution, enormous efforts have been devoted to presenting clean energy sources as candidates to replace fossil fuels. Among them, hydrogen energy, as a carbon

free energy carrier with the highest energy density (146 kJ g^{-1}), has been considered as a next-generation energy source.[1,2]

Currently, hydrogen is mostly produced by steam reforming of natural gas in industry, which not only consumes fossil fuels but also emits carbon dioxide (CO_2) gas leading to the greenhouse effect.[3] Thus, electrochemical water splitting, as a carbon-zero process for producing H_2, has recently attracted huge attention.[4,5] In order to realize the carbon-zero process for commercial scale hydrogen production, development of efficient electrocatalysts for water splitting is considered as one of the most critical challenges.[6]

Although Pt is the most efficient catalyst for the hydrogen evolution reaction (HER), it has intrinsic limitations for widespread applications due to its towering cost, scarcity and instability.[7]

[a] School of Energy and Chemical Engineering, Center for Dimension-Controllable Organic Frameworks, Ulsan National Institute of Science and Technology (UNIST), 50 UNIST, Ulsan 44919, South Korea. E-mail: jbbaek@unist.ac.kr; Fax: +82-52-217-2019; Tel: +82-52-217-2510

[b] Department of Chemical Engineering, Wonkwang University, 460, Iksandae-ro, Iksan, Jeonbuk 54538, South Korea

Seo-Yoon Bae is a post-doctoral fellow in the School of Energy and Chemical Engineering, Center for Dimension-Controllable Organic Frameworks, at Ulsan National Institute of Science and Technology (UNIST), South Korea. After receiving her PhD from the same school at UNIST in 2016, she joined a reputable government institute, the Korea Research Institute of Chemical Technology (KRICT) in Ulsan. Her current research involves the synthesis of three-dimensional porous carbon-based materials for energy applications.

Seo-Yoon Bae

Javeed Mahmood is research assistant professor in the School of Energy and Chemical Engineering, Center for Dimension-Controllable Organic Frameworks, at Ulsan National Institute of Science and Technology (UNIST), South Korea. He received his PhD from the School of Energy and Chemical Engineering at UNIST in 2015 (South Korea). His current research interest includes the design and synthesis of novel fused organic frameworks and their transition metal hybrids for practically important applications.

Javeed Mahmood

To realize hydrogen economy, the development of cheap, efficient and durable electrocatalysts is essential. Over the past few decades, tremendous efforts have been dedicated to finding promising alternatives to Pt-based catalysts, including non-precious-metal-based catalysts and metal-free-based catalysts. However, they are much inferior to Pt-based catalysts, exhibiting higher overpotentials and lower durability.[7,8]

Moreover, to date, most of the research studies on Pt-based electrocatalysts, showing excellent HER performance, have focused on acidic media. In neutral or alkaline solutions, the activity of Pt is generally about 2–3 orders of magnitude lower than that under acidic conditions,[9] because of its sluggish kinetics by slow water dissociation in alkaline solution.[10] The development of catalysts working well at all pH values is indispensable for wide practical applications.

Very recently, ruthenium (Ru) with 1/5 the price of Pt metal[11] has attracted huge attention as a promising electrocatalyst as an alternative to Pt for the HER. It has shown intrinsic HER performance comparable to or even better than that of Pt, and possesses a similar bond strength with hydrogen ($\sim$65 kcal mol^{-1}), which is directly related to the HER activity in neutral or alkaline electrolytes.[11,12] Furthermore, for water dissociation and chemisorption of OH, Ru has shown superior performance to other metals.[11–13]
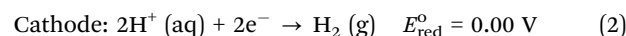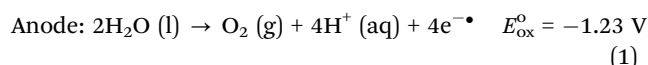
Despite the attractive properties of Ru, studies associated with Ru-based catalysts for the HER are still in their infancy. Thus, research studies of Ru-based catalysts for scientific understanding and systematic strategies for design and synthesis are rare. Therefore, an overview of the recent progress in Ru-based materials for the HER is necessary. In this review, recently developed Ru-based electrocatalysts with outstanding HER performance are summarized. Firstly, we briefly introduce the basic principle of the HER for scientific understanding. Then, various HER catalyst families based on their components, *i.e.*, Ru catalysts on carbon materials, Ru phosphide

based catalysts, and Ru catalysts with transition metals, are reviewed. Finally, we will discuss the challenges and perspectives of Ru-based materials in the HER research field.

## 2. Basic principles of the hydrogen evolution reaction

Theoretically, the water splitting reaction (decomposition of H_2O) takes place at a thermodynamic voltage of 1.23 V, corresponding to an energy of 237.2 kJ mol^{-1}, at 25 °C and 1 atm.[14] However, to achieve electrochemical water splitting in a practical process, a larger voltage than 1.23 V is required due to complicated electron and ion transfer processes leading to sluggish kinetics and low energy efficiency.[15] An additional potential, called the overpotential (η), over the theoretical reaction voltage results from unfavorable factors such as activation energy, electrolyte diffusion blockage, ion and gas diffusion, wire and electrode resistance, and bubble resistance.[2] Many research studies have been conducted to reduce the overpotential through improving the disadvantageous factors. Among various approaches, the research for seeking appropriate electrocatalysts having an adequate interaction with hydrogen and water molecules has attracted huge attention, because appropriate catalysts could dramatically decrease the overpotential and improve the reaction rate and efficiency. Although the electrochemical water splitting reaction consists of the anodic oxygen evolution reaction (OER, eqn (1) and (3)) and the cathodic hydrogen evolution reaction (HER, eqn (2) and (4)), in this review we focus on the HER.

Acidic media:

$$\text{Anode: } 2H_2O \text{ (l)} \rightarrow O_2 \text{ (g)} + 4H^+ \text{ (aq)} + 4e^{-\bullet} \quad E^o_{ox} = -1.23 \text{ V} \tag{1}$$

$$\text{Cathode: } 2H^+ \text{ (aq)} + 2e^- \rightarrow H_2 \text{ (g)} \quad E^o_{red} = 0.00 \text{ V} \tag{2}$$
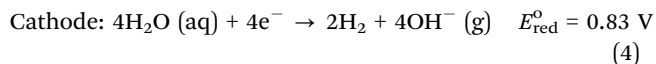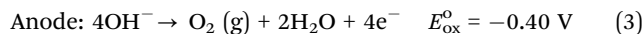
In-Yup Jeon is an assistant professor in the Department of Chemical Engineering, Wonkwang University, South Korea (2017). After receiving his PhD from Ulsan National Institute of Science and Technology (UNIST) (South Korea, 2013), he worked as research associate at UNIST until 2017. His current research interests include the synthesis and chemical modification of carbon nanomaterials for multifunctional applications.

In-Yup Jeon
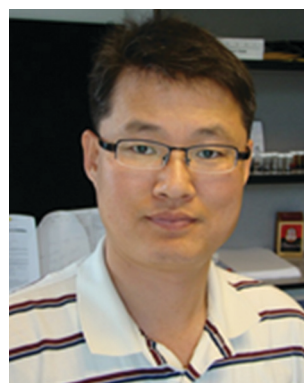
Jong-Beom Baek is a professor and director of the School of Energy and Chemical Engineering, Center for Dimension Controllable Organic Frameworks, at Ulsan National Institute of Science and Technology (UNIST), South Korea. After receiving his PhD from the University of Akron, USA (Polymer Science, 1998), he joined the Wright-Patterson Air Force Research Laboratory (AFRL). He returned to South Korea to take a position as an assistant professor at Chungbuk

Jong-Beom Baek

National University in 2003, before moving to UNIST in 2008. His current research interests include the synthesis of two-dimensional high-performance polymers and chemical modification of carbon-based materials for multifunctional applications.

Alkaline media:

Anode: $4OH^- \rightarrow O_2 \ (g) + 2H_2O + 4e^-$ $E^o_{ox} = -0.40 \ V$ (3)

Cathode: $4H_2O \ (aq) + 4e^- \rightarrow 2H_2 + 4OH^- \ (g)$ $E^o_{red} = 0.83 \ V$ (4)

For the synthesis and design of outstanding electrocatalysts, an understanding of the water splitting HER process is essential. Possible reaction pathways for the HER are composed of a two-step process,[16,17] including production of an adsorbed hydrogen atom (Cat–H, H*) on the surface of the catalyst through the Volmer step and formation of H_2 through the Tafel step or the Heyrovsky step or both (Table 1). The HER could happen through either the Volmer–Heyrovsky or the Volmer–Tafel mechanism. The rate of the hydrogen generation reaction is greatly dependent on the pH value of the electrolyte for both alkaline liquid electrolyte water electrolysis (ALKWE) and acid liquid electrolyte water electrolysis (ACIWE) processes.[18] Particularly, in alkaline solution, the whole reaction rate is influenced by the Volmer step due to the requirement of an additional water dissociation step.[16,19] Although Ru-based catalysts having outstanding HER performance in alkaline medium have been recently reported, the understanding of the mechanism of the HER in basic solution is still obscure. For various Ru-based catalyst research studies, an additional mechanistic study on alkaline electrolytes is essential.

For the formation of hydrogen, hydrogen dissociation (Volmer step) is always involved in the HER process. Consequently, the DFT calculated Gibbs free energy of hydrogen adsorption (ΔG_{H^*}) as a descriptor has been generally used to support experimental results.[8,20,21] According to Sabatier's principle,[22] the ΔG_{H^*} would be ideally zero for a good HER catalyst,[23] which means that the hydrogen binding energy of the catalyst should be neither too weak nor too strong. If the hydrogen bond on the surface of the catalyst is too weak, the catalyst is not sufficiently activated, while if the hydrogen bond with the catalyst is too strong, most of the catalytic active sites are occupied (poisoning effect).[24,25]

Besides the DFT calculation of ΔG_{H^*}, binding energies of H_2O and OH have been considered to understand the phenomena in alkaline solution.[16,19] However, to date, theoretical research of binding energies of H_2O and OH has been rare. For a systematic understanding of Ru-based catalysts, additional theoretical studies are necessary.

3. Ru catalysts with carbon supports

3.1 Ru catalysts on carbon supports

Carbon materials, such as carbon nanotubes, graphene, activated carbon, heteroatom-doped carbon, have received huge attention as catalytic supports in the field of HER. It is because of their capability to increase exposed active sites by controlling the morphology of carbon nanostructures with high specific surface area and boosting the electrical conductivity to efficiently facilitate electron transfer. Moreover, catalytic activity can be improved by forming strong interactions with catalytic metal nanoparticles, preventing aggregation of particles during fabrication and the electrochemical reaction. More importantly, the durability of catalysts can be enhanced by protecting the nanoparticles from the electrolyte.[26]

Recently, many attempts have been dedicated to fabricating Ru based carbon hybrid composites using graphene or graphitic structures. As a consequence of various efforts, the hybrid materials exhibit outstanding electrocatalytic activity toward the HER. Baek et al.[27] developed mass producible Ru nanoparticles (~2 nm) uniformly dispersed on graphene nanoplatelets (Ru@GnP), which exhibited outstanding HER performance in both acidic and alkaline electrolytes. To produce Ru@GnP (Fig. 1a), edge-carboxylic acid functionalized graphene nanoplatelets (CGnPs) were first prepared via ball-milling graphite in the presence of dry ice.[28] The resultant CGnPs can provide high crystalline basal planes for enhanced electrical conductivity and numerous carboxylic acid groups for easily anchoring metal ions. Anchoring Ru ions on CGnPs was carried out in an aqueous medium and subsequent thermal annealing reduced Ru ions into Ru nanoparticles. In this system, CGnPs as catalytic supports play several critical roles in improving the HER performance,[26] such as offering reactive sites with Ru ions, increasing catalytic active sites by high specific surface area ($403.04 \ m^2 \ g^{-1}$), preventing the aggregation of Ru nanoparticles, and hence enhancing the durability of Ru@GnP. The as-prepared Ru@GnP showed low Tafel slopes (Fig. 1b and d) ($30 \ mV \ dec^{-1}$ in 0.5 M H_2SO_4, $28 \ mV \ dec^{-1}$ in 1 M KOH), small overpotential (Fig. 1c and e) at $10 \ mA \ cm^{-2}$ (13 mV in 0.5 M H_2SO_4, 22 mV in 1 M KOH), and long-term durability in both acidic and alkaline media. Interestingly, in the case of Ru on nitrogen doped GnP (Ru@NGnP), which was prepared by post heat-treatment of Ru@CGnP/dicyanodiamine, the catalytic activity of randomly nitrogen doped Ru@NGnP was significantly reduced. It was because the metal-centered active sites

Table 1 Overall possible reaction pathways for the HER

Condition	Overall reaction	Step	Reaction pathway
Acidic	$2H^+ + 2e^- \rightarrow H_2$	Volmer	$H^+ + e^- + Cat \rightarrow Cat–H$
		Heyrovsky	$H^+ + e^- + Cat–H \rightarrow H_2 + Cat$
		Tafel	$Cat–H + Cat–H \rightarrow H_2 + 2Cat$
Alkaline & neutral	$2H_2O + 2e^- \rightarrow H_2 + 2OH^{-\bullet}$	Volmer	$H_2O + e^- + Cat \rightarrow Cat–H + OH^-$
		Heyrovsky	$H_2O + e^- + Cat–H \rightarrow H_2 + OH^- + Cat$
		Tafel	$Cat–H + Cat–H \rightarrow H_2 + 2Cat$

Cat: catalyst, Cat–H: adsorbed hydrogen atom on the surface of the catalyst.
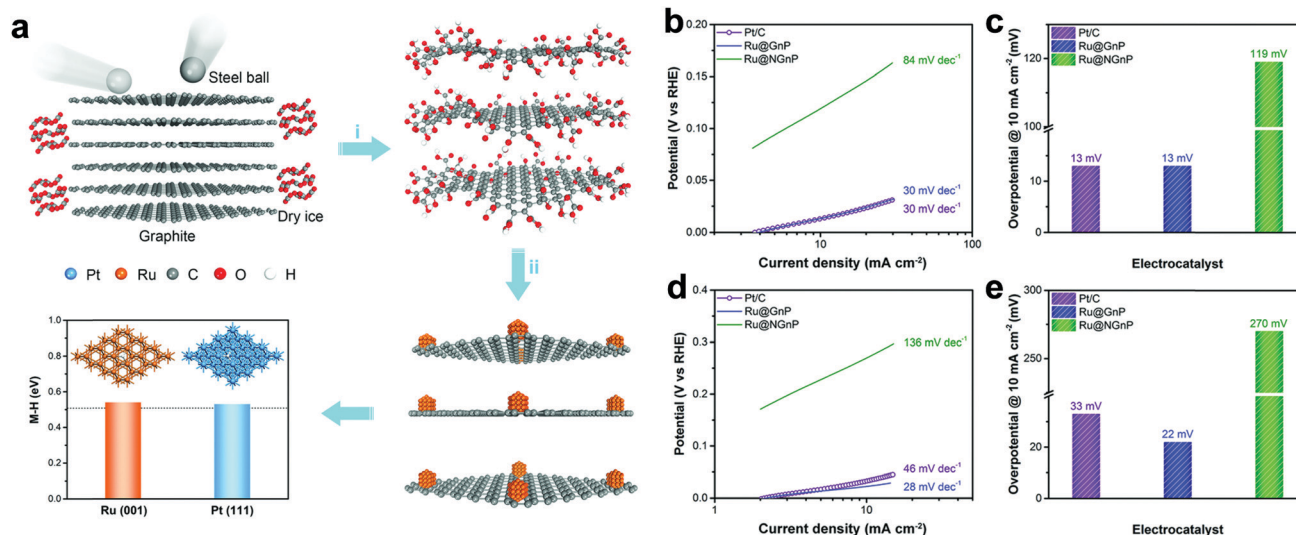
Fig. 1 (a) Schematic illustration of the synthesis of Ru@GnP and theoretical calculation of hydrogen binding energies of Ru(001) and Pt(111). (i) Physical cracking of graphite through the ball-milling method. (ii) *In situ* formation Ru@CGnP through reduction of Ru ions and annealing. (b and d) Tafel plots of Ru@GnP, Ru@NGnP, and Pt/C in 0.5 M H_2SO_4 (b) and in 1.0 M KOH (d) solutions. (c and e) Overpotential of Ru@GnP, Ru@NGnP, and Pt/C at a current density of 10 mA cm^{-2} in 0.5 M H_2SO_4 (c) and in 1.0 M KOH (e) solutions.[27]

were blocked by the formation of Ru–N coordination. The Ru@GnP catalyst prepared by simple mechanochemical synthesis suggests scalable production for practical applications. Chen *et al.*[29] developed a facile route to synthesize graphene-like layered carbon (GLC) from a layered silicate template as a supporting material for the uniform loading of Ru nanoparticles. The GLC played a crucial role in uniformly dispersing the Ru nanoparticles due to the affinity of GLC with Ru nanoparticles. The highest loading amount of Ru nanoparticle in GLC is 62 wt% without agglomeration. The Ru/GLC (10 wt%) composite showed outstanding electrocatalytic activity for the HER with a small Tafel slope of 46 mV dec^{-1}.

As another synthesis strategy, metal–organic frameworks (MOFs) having organic ligands to form a highly ordered crystal structure have been widely used due to the high surface area and uniform distribution of the metal nanoparticles.[30,31] Qiu *et al.*[32] reported a novel strategy for synthesis of Ru-based electrocatalysts with abundant Ru active sites using bimetallic MOFs through pyrolysis and etching of Cu. To prepare a Ru-based catalyst, they used bimetallic CuRu–MOF as the template, leading to ultrafine Ru nanoparticles and abundant meso/macropores generated from the removal of Cu particles. The as-prepared ultrafine Ru nanoparticles anchored on hierarchically porous carbon (Ru–HPC) showed outstanding HER activity with a low Tafel slope of 33.9 mV dec^{-1} in 1 M aq KOH solution, which is superior to that of Pt/C (20 wt%).

3.2 Ru catalysts on nitrogen-doped carbon

To enhance the catalytic activity, heteroatoms, such as nitrogen (N), phosphorus (P), sulphur (S), and boron (B), have been introduced into carbon materials. Introduction of these heteroatoms in carbon materials could modulate the chemical activity of carbon-based composites by their electron-donating/accepting properties.[33,34] Interestingly, among heteroatoms, nitrogen has similar atomic size to carbon.[35] Hence, the electronic structures

of carbon composites through nitrogen doping could be easily modulated, minimizing the lattice disorder. Due to such a strong point of N-doped carbon, Ru based hybrids with N-doped carbon have shown excellent HER activity.[11,35,36]

Interestingly, recent research studies reported that Ru-based catalysts showed superior performance in alkaline electrolytes. Although the understanding of these catalysts from the calculation of Gibbs free energy under acidic conditions is quite complete with supporting experimental results, it is insufficient under basic conditions. Thus, a few reports have studied the feasibility of water dissociation on the surfaces of Ru-based catalysts to elucidate specific properties. Mahmood *et al.*[12] prepared Ru nanoparticles dispersed within a nitrogenated holey two-dimensional carbon structure (Ru@C_2N) for the HER under both acidic and basic conditions (Fig. 2a). C_2N was synthesized *via* a one-pot polycondensation reaction between hexaaminobenzene (HAB) trihydrochlride and hexaketo-cyclohexane (HKH) in the presence of ruthenium chloride (RuCl$_3$), which has a uniform structure with six nitrogen atoms facing each other in evenly distributed periodic holes (0.83 nm), providing a large surface area, a conductive platform and anchoring sites. The electrocatalytic activity of Ru@C_2N was compared with other metal nanoparticles with C_2N such as Co@C_2N, Ni@C_2N, Pd@C_2N, and Pt@C_2N in a 0.5 M aq. H_2SO_4 solution and in 1.0 M aq. KOH solution. The Ru@C_2N showed outstanding electrocatalytic performance such as high turnover frequencies (TOF) at 25 mV (0.67 H_2 s^{-1} in 0.5 M H_2SO_4 and 0.75 H_2 s^{-1} in 1.0 M KOH), small overpotentials at 10 mA cm^{-2} (13.5 mV in 0.5 M H_2SO_4; 17.0 mV in 1.0 M KOH), and superior durability in both electrolytes. These performances are comparable to, or even better than, that of the Pt/C catalyst for the HER in a wide range of pH values. Meanwhile, the performance of Ru@C_2N is contradictory to that of Ru@NGnP,[27] which demonstrated reduced electrocatalytic activity after nitrogen
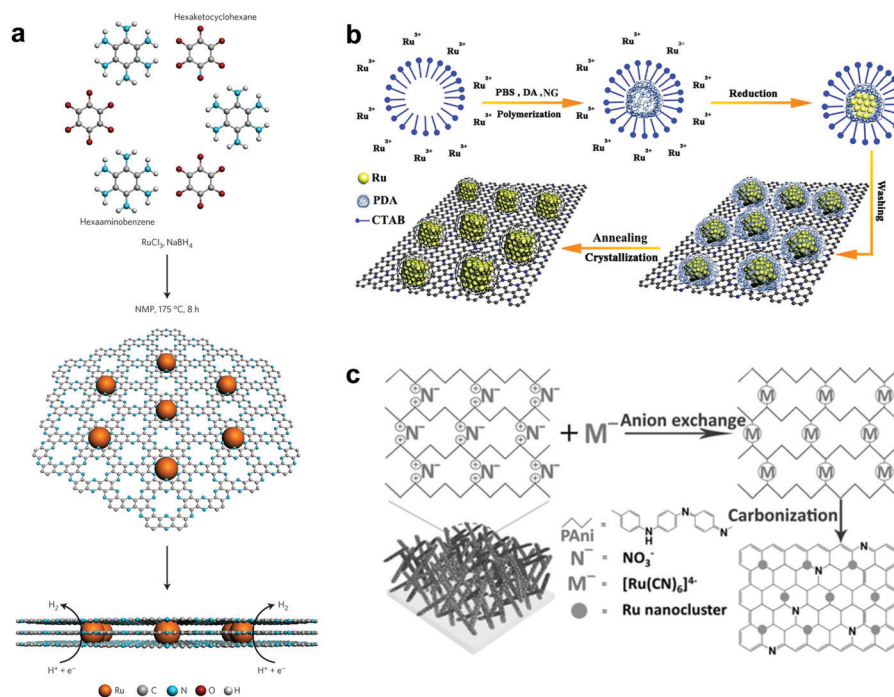
Fig. 2 Schematic illustrations of various synthesis procedures and structures of Ru based catalysts with nitrogen doped carbon (NC): (a) Ru@C$_2$N[12] through a condensation reaction, (b) hcp-Ru@NC[36] on nitrogen-doped graphene (NG) through self-assembly and thermal annealing, (c) Ru@NC[37] through an electrochemical method.

doping, because of the difference in particle size and uniformity caused by different synthesis approaches. For example, in the case of Ru@NGnP, Ru@GnP should be formed first and then post heat-treated in the presence of a nitrogen precursor. In this case, the available catalytic active sites could be blocked by the nitrogen source. To understand the high electrocalalytic activity of Ru@C$_2$N active sites during hydrogen evolution in both solutions, they calculated the binding energy of H$_2$O, H, and OH with Pt$_{55}$, Ru$_{55}$, and Ru$_{55}$@C$_2$N. From all bonding points of view, Pt is the best candidate for the HER in alkaline solution with moderate H (0.60 eV) and low OH (−0.49 eV) binding energies. In the case of Ru$_{55}$, although H$_2$O and H binding energies are similar to those of Pt$_{55}$, the OH binding energy is much higher than that of Pt$_{55}$, which leads to a decrease in HER efficiency. However, the Ru$_{55}$ anchored on C$_2$N (top: 0.69 eV, near surface 1.45 eV) showed much higher H$_2$O binding energy than Ru$_{55}$ (0.58 eV) and Pt$_{55}$ (0.59 eV). In other words, the strong attraction to H$_2$O can accelerate the rate of H$_2$O capture and dissociation of H$_2$O into H and OH, leading to a much faster proton supply. Consequentially, the Ru$_{55}$@C$_2$N overcomes the efficiency loss from high OH binding energy (top: 0.46 eV, near surface: 0.53 eV) through the highest H$_2$O binding energy, and exhibits superior HER performance to Pt$_{55}$ and Ru$_{55}$. Wang et al.[38] prepared Ru nanoparticles (∼2.37 nm, 3.14 wt%) highly dispersed on N-doped carbon (Ru@CN) via a one-pot solid-state pyrolysis method using glucosamine hydrochloride, melamine and RuCl$_3$. The as-prepared catalyst exhibited remarkable activity for the HER over wide pH and temperature ranges, vastly broadening applications. Particularly, in alkaline solution,

Ru@CN showed much higher electrocatalytic activity than Pt because of the negligible energy barrier for H$_2$O dissociation on Ru. Interestingly, for H$_2$O dissociation in basic media, Ru undergoes an exothermic process, whereas Pt follows an endothermic process (Fig. 3). Liu et al.[39] reported a computational study on Pt and Ru dimers on defective graphene (DG) and nitrogen doped graphene (NG) to understand the relationship between various descriptors including the free energies of H* (ΔG_{H*}) and OH* (ΔG_{OH*}), the kinetic barriers of water dissociation (E_a) and the dissociative chemisorption energy of water (ΔE_{diss}). Among six structural models of metal dimers, PtRu@NG showed an optimal ΔG_{H*} (−0.07 eV) for the HER under acidic conditions (pH = 0). Under alkaline conditions (pH = 14), a linear correlation between ΔE_{diss} and E_a in Brønsted–Evans–Polanyi (BEP) type relationships was observed, because ΔE_{diss} was linearly correlated with the d-band center of the metals.[40]

Qiao et al.[11] considered the effect of difference in crystal structures of Ru between face-centered cubic (fcc) and hexagonal-closed packed (hcp) structures. They reported development of Ru nanoparticles with a new face-centered cubic (fcc) crystallographic structure, which shows 2.5 times higher hydrogen evolution rate than Pt in alkaline solution. To prepare anomalous fcc structured Ru (Ru$_{fcc}$), g-C$_3$N$_4$ as a catalytic support plays a crucial role in the formation of Ru$_{fcc}$ achieved by enhanced metal–substrate interactions and a nanosize effect of Ru. Based on DFT calculations (Fig. 4), they demonstrated the superiority of Ru$_{fcc}$ as a catalyst for hydrogen generation over hcp structured Ru (Ru$_{hcp}$), generally a dominant structure in Ru,[41] and over commercial Pt/C. When water dissociation
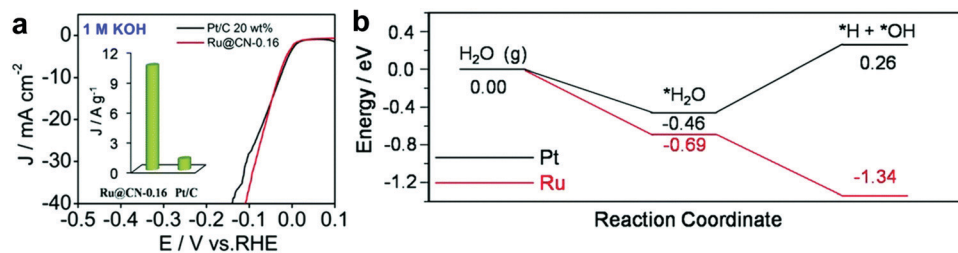
Fig. 3 (a) Polarization curves of Ru@CN-0.16 and Pt/C (inset: the mass activity of Ru@CN-0.16 and Pt/C). (b) A schematic energy diagram of the energy regarding the reaction coordinates for water dissociation.[38]

kinetics from the Volmer step is considered, the energy barrier of the Ru_{fcc} surface ($\Delta G_B = 0.41$ eV) is lower than that of Ru_{hcp} ($\Delta G_B = 0.51$ eV) and Pt/C ($\Delta G_B = 0.94$ eV). Therefore, Ru_{fcc} shows outstanding electrocatalytic performance with a high TOF of 4.2 s^{-1} at an overpotential of 100 mV in alkaline solutions.

As a general strategy, pyrolysis of polymers and other organic materials at high temperature is wildly used for heteroatom doping and thus increasing electrical conductivity. Lu et al.[42] fabricated a Ru and nitrogen codoped carbon nanowire (Ru–NC) by four-step reaction sequences, hydrothermal treatment of tellurium nanowires (Te NWs), formation of a melamine-formaldehyde (MF) resin shell on Te NWs, incorporation of the Ru precursor into Te@MF, and pyrolysis of the Ru–MF NW at various elevated temperatures. Among heat-treated Ru–NC, Ru–NC-700 (heat-treated at 700 °C) exhibited the best HER performance with the lowest overpotential (12 mV) at 10 mV cm^{-2} and Tafel slope (14 mV dec^{-1}). Zhang et al.[43] prepared a novel ruthenium/nitrogen-doped carbon (Ru/NC) electrocatalyst supported by graphite foam through in situ thermal annealing of Ru^{3+}/polyaniline on graphite foam at 900 °C under a nitrogen atmosphere. The resultant Ru/NC catalyst exhibited excellent electrocatalytic activity in 1 M aq. KOH solution with a low overpotential (21 mV at 10 mA cm^{-2}). Li et al.[36] fabricated ordered hexagonal-closed packed (hcp)-Ru nanoparticles with an N-doped carbon (NC) shell through a surfactant-assisted self-assembly and polydopamine-reduction process using $RuCl_3 \cdot 3H_2O$ (Fig. 2b). The as-prepared RuNP@PDA was anchored on a carbon support and carbonized at 700 °C for enhanced HER performance through improving its crystallinity.

The in situ formed NC from polydopamine prevented the agglomeration of Ru nanoparticles during the annealing process. The hcp-Ru@NC catalyst showed a small overpotential (27.5 mV at 10 mA cm^{-2}), small Tafel slope (34 mV dec^{-1}) and long-term durability in an acidic electrolyte. Furthermore, using pyrolysis of carbon foam with abundant nitrogen sources and large surface area as a way to synthesize the core–shell structure,[44] Song et al.[45] prepared metal nanoparticles coated with graphite carbon (GC) with large surface area and carbon with abundant nitrogen. Ru nanoparticles encapsulated in nitrogen-doped graphite carbon materials (Ru-NGC) in carbon foam were fabricated by slow thermal pyrolysis at 800 °C. Additionally, they prepared Ni and Co encapsulated in NGC. Among them, Ru-NGC showed better HER activity with a low Tafel slope (31 mV dec^{-1}), small overpotential of 25 mV at a current density of 10 mV cm^{-2} and high TOF (0.68 H_2 s^{-1}) in 0.5 M H_2SO_4.

Besides the pyrolysis method, using a simple electrochemical method, Li et al.[37] developed mono-dispersed Ru nanoclusters in a hierarchically ordered carbon electrode (Fig. 2c). To make a hierarchically ordered carbon structure, they used polyaniline composed of quinonoid imine (QI) and benzenoid amine (BA); the ratio of QI and BA can be reversibly controlled by an externally applied potential.[46] Interestingly, QI groups can more strongly bond with Ru ions than BA, because of the selective ion-bonding effect. Based on the properties of polyaniline, Ru@NC having a low loading of about 2 wt% Ru was prepared, which showed outstanding activity with a low Tafel slope of 36 mV dec^{-1} and excellent durability in 1 M aq. KOH solution.
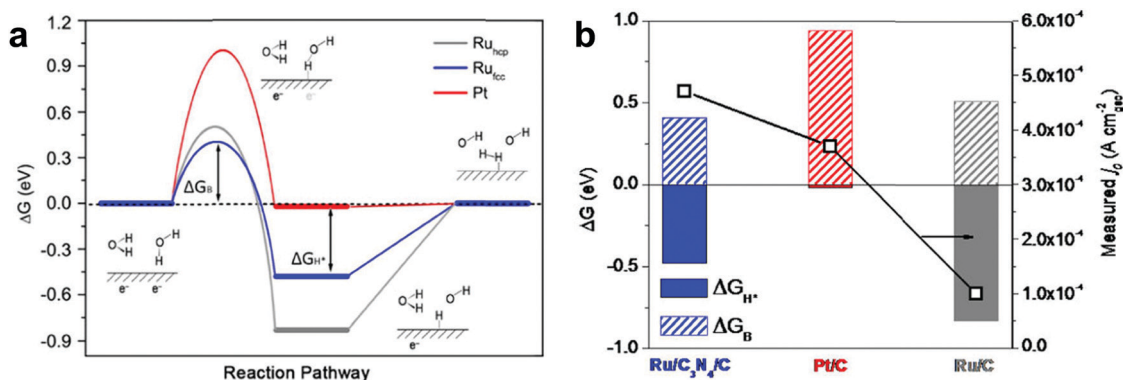

Fig. 4 (a) Gibbs free energy diagram of the HER (ΔG_{H^*}: hydrogen adsorption free energy, ΔG_B: water dissociation free energy barrier). (b) The relationship between the computed ΔG_{H^*} or ΔG_B values and the measured j_0 values on various metal surfaces.[11]

Table 2 Summary of HER performance of Ru catalysts with carbon materials

Reaction medium	Catalyst	Loading density ($\mu g\ cm^{-2}$)	Tafel slope ($mV\ dec^{-1}$)	Overpotential at 10 mA cm^{-2} (mV)	Ref.
1.0 M KOH	Ru-NC-700	200	14	12	42
	Ru@GnP	250	28	22	27
	Ru/NC		31	21	43
	Ru-HPC	200	33.9	22.7[a]	32
	Ru@NC	300	36	26	37
	Ru@C$_2$N	285	38	17	12
	Ru-NGC	360	40		45
	Ru@CN	245	53	32	38
	Ru/C$_3$N$_4$/C	204		79	11
0.5 M H$_2$SO$_4$	Ru@GnP	750	30	13	27
	Ru@C$_2$N	285	30	13.5	12
	Ru/GLC	400	30	35	29
	Ru-NGC	360	31	25	45
	hcp-Ru@NC-700	280	37	27.5	36
	Ru-HPC	200	66.8	61.6	32

[a] Overpotential at a current density of 25 mA cm^{-2}.

The HER performances of recently reported Ru catalysts on carbon materials are summarized in Table 2.

4. Ru phosphide-based catalysts

Theoretically, phosphorus (P) has been considered as a proton acceptor for the initiation of the HER, due to its unique electron-distribution.[47,48] According to previous studies on transition metal phosphides (TMPs), such as MoP,[49] FeP,[50] CoP,[51] and Ni$_2$P,[52] the capability of phosphorus for hydrogen generation has been demonstrated. Based on its potential, research studies regarding Ru phosphides as catalysts for the HER have been recently reported.

Depending on the combination between Ru and P, changes in the electronic and physicochemical properties of RuP$_x$ occur.[53–55] Several recent studies related to Ru phosphide have shown the difference in HER activity according to the difference in the ratio of Ru and P. Chang et al.[56] reported the influence of P content on the HER activity of Ru phosphides. They prepared two kinds of Ru phosphides, RuP and RuP$_2$, via simple thermal decomposition using ruthenium chloride (RuCl$_3$) and hypophosphite (NaH$_2$PO$_2$). During the thermal treatment in hydrogen gas in the temperature range from 425 to 600 °C, P-rich RuP$_2$ was formed above 500 °C and P-poor RuP was formed below 500 °C. They compared the HER performances of 550 °C heat-treated RuP$_2$ (RuP$_2$-550) and 475 °C heat-treated RuP (RuP-475) at all pH values. Interestingly, in the case of RuP-475 with more Ru, the electrocatalytic activity was apparently improved at all pH values. RuP-475 has much more electrocatalytic active sites and better conductivity than the P rich RuP$_2$-550 due to P atom[57] with slightly high electronegativity disturbing the electron delocalization in the metal. Liu et al.[58] introduced the effect of content of phosphate in Ru phosphide for improving the HER activity. They prepared three kinds of Ru phosphides (Ru$_2$P, RuP, and RuP$_2$) with similar dimensions, morphology, and surface area on graphene nanosheets through controlling the amount of phytic acid (PA)

as the P source, and compared the three kinds of Ru phosphides. Among them, Ru$_2$P/graphene showed the best HER activity with a low Tafel slope of 32 mV dec^{-1} in an acidic electrolyte. To understand these tendencies, they calculated the Gibbs free energy of hydrogen adsorption (ΔG_{H^*}) of the three materials. Ru$_2$P has a (ΔG_{H^*}) of 0.164 eV, which is lower than those of RuP (−0.198 eV) and RuP$_2$ (−0.428 eV). The theoretical result is in good agreement with experimental results.

As a general strategy to enhance the activity and stability of HER catalysts, carbon materials have been introduced in metal catalysts. Liu et al.[59] reported the preparation of Ru phosphide nanoparticles supported on reduced graphene oxide (RGO) nanosheets (Ru$_2$P/RGO-20) via a two-step procedure. First, the nucleation of Ru(III) nanoparticles from RuCl$_3$ on graphene oxide (GO) in aqueous solution and subsequently phosphidation of Ru nanoparticles using NaH$_2$PO$_2$ at 600 °C were carried out. The as-prepared Ru$_2$P/RGO-20 (overpotential of −22 mV under acidic conditions, overpotential of −13 mV under basic conditions at a current density of −10 mA cm^{-2}) exhibited higher catalytic activity and better durability than the Pt/C catalyst in both acidic and alkaline solutions. Additionally, to estimate the Gibbs free energy of hydrogen adsorption (ΔG_{H^*}), theoretical analysis through DFT calculations was also conducted. The Ru$_2$P(112) hollow site (−0.31 eV)[60] was demonstrated as the most favorable H adsorption site. When some electrons are transferred from Ru to the sp^2 carbon surface (Ru$_2$P/RGO-20), the value of ΔG_{H^*} increases to 0.058 eV. The value of Ru$_2$P/RGO-20 is even better than that of Pt (−0.09 eV). The DFT calculation results support the measured electrocatalytic activity for the HER.

Moreover, N and P dual doped carbon having a low electronegativity could be coupled with highly active RuP$_x$. It may cause a reduction of the hydrogen binding energy,[62,63] consequently leading to an improvement of electrocatalytic activity for hydrogen evolution. Recently, N and P dual doped carbon encapsulated Ru diphosphide nanoparticles (RuP$_2$@NPC) were fabricated by Pu et al.[61] The catalyst was prepared using a self-assembled phytic acid cross-linked Ru complex (RuPA) and melamine via pyrolysis at 900 °C (Fig. 5). From computational
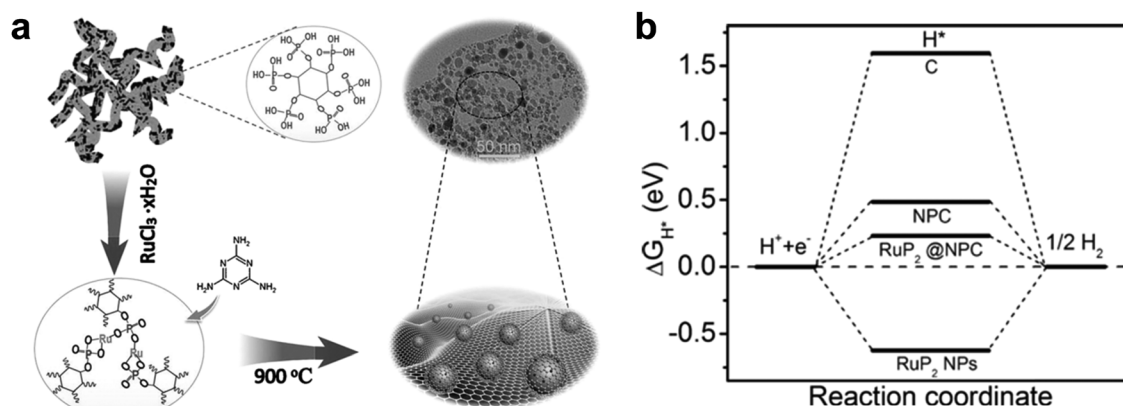
Fig. 5 (a) Schematic illustration of the synthesis of the RuP$_2$@NPC. (b) The calculated free-energy diagram of the HER at equilibrium potential for RuP$_2$@NPC, RuP$_2$ NPs, NPC, and C.[61]

studies, the hydrogen adsorption energy of RuP$_2$@NPC (0.233 eV) is weaker than that of RuP$_2$ (-0.627 eV), which means RuP$_2$@NPC is a better catalyst than RuP$_2$ due to the closer value to 0 eV. The as-prepared RuP$_2$@NPC exhibited outstanding electrocatalytic performance with low Tafel slopes (38 mV dec^{-1} in 0.5 M H$_2$SO$_4$, 87 mV dec^{-1} in 1.0 M aq. phosphate buffer saline (PBS), and 69 mV dec^{-1} in 1.0 M aq. KOH), low overpotentials at 10 mA cm^{-2} (38 mV in 0.5 M H$_2$SO$_4$, 57 mV in 1.0 M aq. PBS, and 52 mV in 1.0 M aq. KOH), and long-term durability at all pH values. The outstanding performance of RuP$_2$@NPC is comparable to that of commercial Pt/C, and the high durability may be due to the NPC encapsulation of RuP$_2$ preventing its corrosion. Chi *et al.*[64] prepared a uniform core–shell hollow nanospherical structure with RuP$_x$ NPs coated with N,P-codoped carbon (RuP@NPC) through copolymerization of aniline–pyrrole and gas phosphorization. The NPC shell can protect aggregation and corrosion of RuP$_x$ in the electrolyte and can enhance the rate of charge-transfer due to the modification of the electronic structures. The optimized RuP$_x$@NPC sample showed a good electrocatalytic performance for the HER in a wide pH range.

As another approach, Yang *et al.*[65] developed uniformly anchored single Ru atoms on phosphorus nitride imide nanotubes (HPN), which is a carbon-free PN matrix. Extremely inhomogeneous electron density of carbon-free PN would facilitate the reaction activation on the substrate, when the PN matrix supports the metal single atom. It is because of its polar P–N bonds and twisted spatial structure.[66] Interestingly, Ru single atoms (SA) can be successfully anchored due to the strong interaction between the d-orbitals of Ru and the lone pair electron of N in the PN support. Ru SAs@PN prepared through a solvothermal reaction and wet impregnation exhibited excellent electrocatalytic activity under acidic conditions with a small Tafel slope of 38 mV dec^{-1} and low overpotential of 24 mV at 10 mA cm^{-2}. In addition, using density functional theory (DFT) calculations, the origin of the superior HER performance of Ru SAs@PN was studied and compared with other catalysts with various supports (Ru SAs@C$_3$N$_4$, Ru SAs@C and Ru/C). The Gibbs free energy of hydrogen adsorption (ΔG_{H*}) of Ru SAs@PN (-0.27 eV) was higher than those of other catalysts.

The HER performances of recently reported Ru phosphide-based catalysts are summarized in Table 3.

5. Ru catalysts on other transition metals

Bimetallic alloy strategies are widely used to improve the electro-catalytic activity through modification of surface properties and

Table 3 Summary of HER performance of Ru phosphide-based catalysts

Reaction medium	Catalyst	Loading density (µg cm^{-2})	Tafel slope (mV dec^{-1})	Overpotential at 10 mA cm^{-2} (mV)	Ref.
1.0 M KOH	RuP-475	348	36	22	67
	Ru$_2$P/RGO	1000	56	13	59
	RuP$_2$@NPC	1000	69	52	61
	RuP@NPC	195	70	74	64
1.0 M PBS	RuP-475	348	45	47	67
	RuP$_2$@NPC	1000	87	57	61
	RuP@NPC	195	59	110	64
0.5 M H$_2$SO$_4$	Ru$_2$P/RGO	1000	29	22	59
	Ru$_2$P/graphene	1000	32	18	58
	Ru SAs@PN	1000	38	24	65
	RuP$_2$@NPC	1000	38	38	61
	RuP-475	348	39	47	67
	RuP@NPC	195	46	51	64

the width of the d-band.[68,69] We will introduce Ru–metal hybrid catalysts for the HER.

5.1. Ru catalysts on precious metals

Among precious metals, palladium (Pd), Pt, and Ru are considered as ideal HER catalysts, because Pd and Pt have outstanding properties of hydrogen atom recombination, while Ru has efficient water dissociation properties.[12,70] In addition, Pt–tellurium (Te) composites have shown superior electrocatalytic performance.[71,72] Based on reported research results, Liu et al.[73] developed novel cation vacancies in a PdPtRuTe five-fold twinned anisotropic structure (v-Pd$_3$Pt$_{29}$Ru$_{62}$Te$_6$ AS) through a facile solid–liquid phase chemical process (Fig. 6). The as-prepared v-Pd$_3$Pt$_{29}$Ru$_{62}$Te$_6$ AS exhibited outstanding HER performance with a low Tafel slope (32 mV dec^{-1} in 0.5 M H$_2$SO$_4$ and 22 mV dec^{-1} in 1.0 M aq. KOH) and the lowest Gibbs free energy of hydrogen adsorption (ΔG_{H^*}) of -0.094 eV. Li et al.[74] developed Ru nanoparticles alloying with even trace amounts of Pt uniformly anchored on a porous carbon sphere (PtRu@RFCS with 0.2 wt% Pt, 5 wt% Ru). The catalyst was simply prepared via the condensation reaction between resorcinol and formaldehyde in the presence of a H$_2$PtCl$_6$ and RuCl$_3$ mixture. The as-prepared PtRu@RFCS with small metal particle size (2.57 nm) and high surface area (S_{BET}: 630.3 m^2 g^{-1}) exhibited superior HER activity in acidic medium with a small Tafel slope (27.2 mV dec^{-1}), a low overpotential at 10 mA cm^{-2} (19.7 mV) and a high TOF (4.03 H$_2$ s^{-1}). The performance of Ru@RFCS is better than that of commercial Pt/C, due to the metallic Pt nanocluster on PtRu alloy nanoparticles, leading to weak bonding with hydrogen and rapid hydrated proton dissociation. Furthermore, the carbon spheres play a crucial role in improving the durability of catalysts, protecting the metals from agglomeration, size growth, detachment, and dissociation. Oh et al.[75] reported a highly active bifunctional electrocatalyst, carbon-supported hollow Pt/NiO/RuO$_2$ (h-PNRO) with an icosahedral skeleton, working on anodic OER and cathodic HER for water splitting. The as-prepared h-PNRO/C showed outstanding activity with a low overpotential (29.6 mV at 10 mA cm^{-2} of current density) and Tafel slope (35 mV dec^{-1}) in 0.1 M aq. HClO$_4$. The enhancement of HER performance can be attributed to increasing the d-band vacancy (ligand effect) which resulted in the alloying of Pt with Ni.[76]

5.2. Ru catalysts on non-precious metals

Various research studies have reported the development of Ru based HER catalysts on non-precious metals, such as cobalt (Co), nickel (Ni), molybdenum (Mo), and cerium (Ce). Xu et al.[77] developed a ruthenium cobalt phosphide hybrid catalyst (RuCoP) obtained by phosphorizing a chemically reduced Ru–Co alloy. The hybrid catalyst showed significant electrocatalytic performance in both acidic and alkaline electrolytes, due to the outstanding partial charge transfer from CoP to Ru and appropriate adsorption energy (E_{ads}) of hydrogen, water, and –OH groups. Based on the density functional theory (DFT) calculations, the adsorption energy of hydrogen of the RuCoP hybrid (-0.52 eV), which is very close to that of Pt (-0.50 eV), leads to the outstanding electrocatalytic performance in acidic media. Weaker E_{ads} of –OH of the RuCoP hybrid (-2.32 eV) than Pt (-2.43 eV) and strong E_{ads} of water of the RuCoP hybrid (-0.92 eV) result in remarkable catalytic activity for the HER in alkaline media. Su et al.[78] fabricated Ru–Co bimetallic nanoalloys encapsulated in nitrogen-doped graphene layers (RuCo@NC) having a small Ru content (3.58 wt%) through the assistance of MOFs and one-step thermal treatment using a Co$_3$[Co(CN)$_6$]$_2$ precursor and RuCl$_3$. This novel catalyst exhibited high catalytic activity realized by the synergistic effect of RuCo alloys and excellent durability over 10 000 cycles due to protection by the carbon cage.[68,79] Furthermore, the theoretical calculation of Gibbs free energy (0.31 eV) of C$_{239}$N$_1$Ru$_3$Co$_{52}$ was consistent with the experimental results. Liu et al.[80] conceived and designed a model of Ru–Ni$_2$P hybrid structure and assessed its ΔG_H via DFT calculations (Fig. 7). The Ru–Ni$_2$P cluster showed energetically favorable adsorption free energy ($\Delta G_H = 0.01$ eV), which is close to the optimal value for hydrogen generation. Based on the DFT calculation results, they developed Ni@Ni$_2$P–Ru heterogeneous nanorods (HNRs) prepared via a simple one-pot synthesis method using RuCl$_3$, trioctyphosphine, oleic acid and 1-dodecylamine. Interestingly, Ru plays a critical role in the formation of the novel nanorods due to a synergistic effect between Ru and Ni and in the improvement of conductivity. The as-prepared HNRs showed outstanding electrocatalytic performance in both acidic and alkaline media (Tafel slopes: 35 mV dec^{-1} and 41 mV dec^{-1} under acidic and alkaline conditions, respectively). Liu et al.[81]
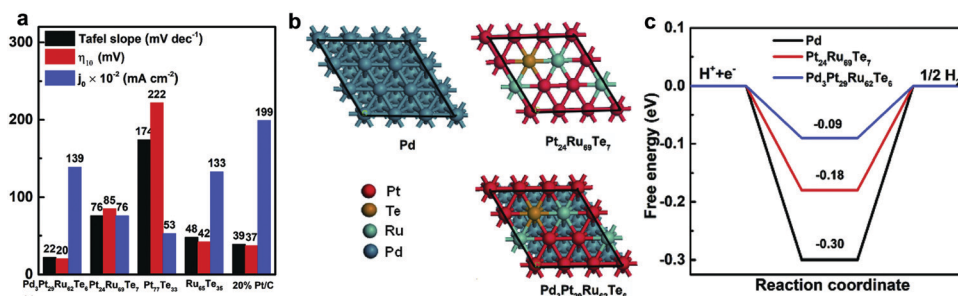

Fig. 6 (a) Overpotential at a current density of 10 mA cm^{-2} (η_{10}), Tafel slopes, and exchange current density (j_0) of v-Pd$_3$Pt$_{29}$Ru$_{62}$Te$_6$ AS and control samples in 1.0 M aq. KOH solutions. (b) Atomic model structures of catalysts, Pd, Pt$_{24}$Ru$_{69}$Te$_7$, and v-Pd$_3$Pt$_{29}$Ru$_{62}$Te$_6$ AS. (c) Calculated free-energy diagram of catalysts.[73]
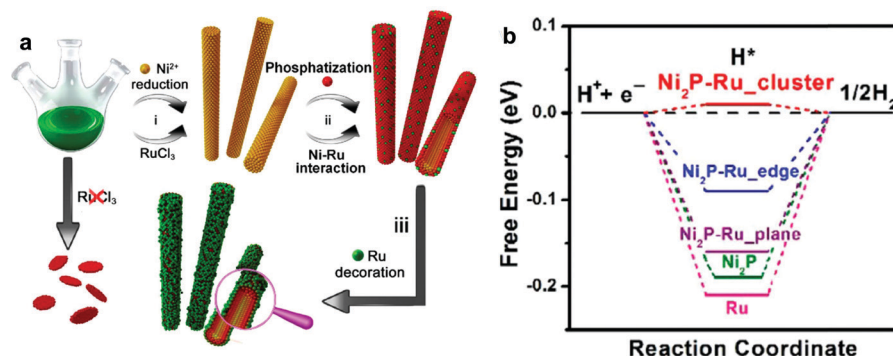
Fig. 7 (a) Schematic illustration of fabrication of Ni@Ni2P–Ru HNRs. (b) Computed free energy diagram of the HER.[80]

fabricated Ru-based catalysts for the HER using MoS_2 having a favorable ΔG_{H^*} (0.08 eV).[82] $Ru-MoS_2$ hybrid nanocomposites on carbon paper ($Ru/MoS_2/CP$) were fabricated *via* a hydrothermal reaction to form vertically aligned MoS_2 nanosheets on CP. The composites were formed by chemical modification using a $RuCl_3$ solution, and further calcination under a H_2 atmosphere. The designed $Ru/MoS_2/CP$ showed outstanding performance (Tafel slope of 60 mV dec^{-1}, overpotential of 13 mV at 10 mA cm^{-2}) in alkaline media due to Ru properties with efficient dissociation of water molecules into OH^- ions. Its high performance stemmed from unsaturated Mo and/or S atoms, which could promote H_{ads} adsorption and their recombination into H_2, and the unique porous morphology of vertically aligned MoS_2 nanosheets, which could provide abundant exposed reaction sites. In addition, Demir *et al.*[83] reported preparation of ceria (CeO_2)-supported Ru^0 nanoparticles (Ru^0/CeO_2) by reduction of Ru^{3+} ions, impregnated on nanoceria, using $NaBH_4$. As a supporting material, ceria has advantages such as favorable interactions with metals[84] and a favorable standard potential (1.76 V) of reduction from Ce^{4+} to Ce^{3+} in acidic media. The hybrid nanocomposite with Ru (1.86 wt%)

exhibited outstanding electrocatalytic performance with a low overpotential (47 mV at 10 mA cm^{-2}) and a small Tafel slope (41 mV dec^{-1}) in acidic medium.

As a unique strategy to prepare electrocatalysts, metal–organic frameworks (MOFs) have been widely used as precursors, due to their high surface area, controllable structure, and tunable porosity.[85,86] Ru-based catalysts with other metals have been fabricated *via* a MOF assisted process. Yuan *et al.*[87] fabricated a series of precious metal clusters (Ru, Pt, and Pd) combining single cobalt atoms anchored on nitrogen-doped carbon (Ru, Pt, Pd@Co-SAs/N-C) made from ZiFs by carbonization and chemical reduction of $RuCl_3 \cdot xH_2O$, H_2PtCl_6, and $PdCl_2$ (Fig. 8). Among them, Ru@Co-SAs/N–C starting from ZnCo-ZIF exhibited excellent electrocatalytic activity and durability in all pH ranges. Particularly, in 1 M aq. KOH solution, the catalytic activity of Ru@Co–SAs/N–C with a low Tafel slope of 30 mV dec^{-1} and an overpotential of 7 mV at 10 mA cm^{-2} is better than that of Pt/C. Xu *et al.*[88] developed low-ruthenium containing NiRu alloy nanoparticles encapsulated in nitrogen-doped carbon by Ru doping in Ni-based metal–organic frameworks (MOF) followed by annealing at 800 °C under a nitrogen atmosphere. The prepared N-doped
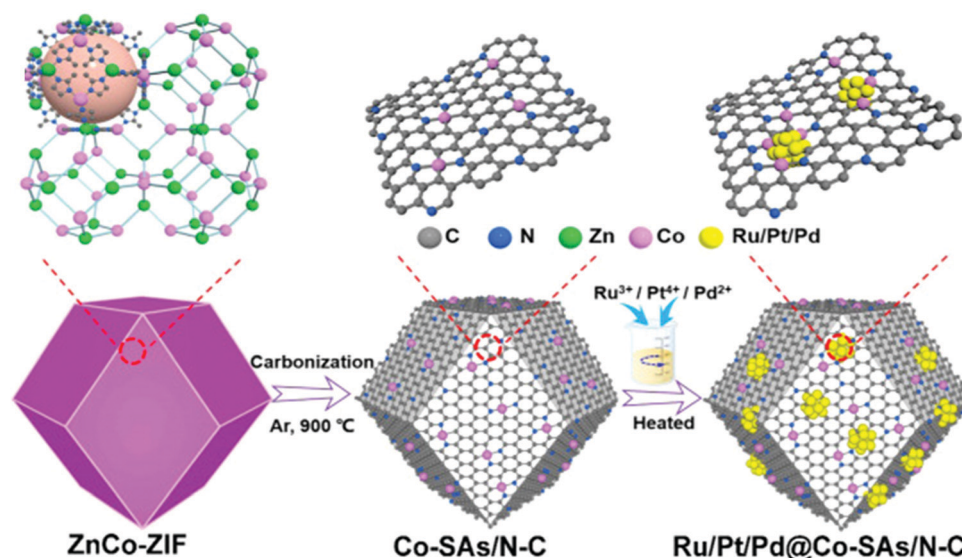

Fig. 8 Schematic diagram of Ru/Pt/Pd@Co-SAs/N-C synthesis.[87]

Table 4 HER performance of Ru catalysts on transition metals

Reaction medium	Catalyst	Loading density ($\mu g\ cm^{-2}$)	Tafel slope ($mV\ dec^{-1}$)	Overpotential at 10 mA cm^{-2} (mV)	Ref.
1.0 M KOH	v-Pt$_{29}$Pd$_3$Ru$_{62}$Te$_6$ AS	285	22	20	73
	Ru@Co–SAs/N–C	285	30	7	87
	RuCo@NC	275	31	28	78
	Ru–MoO$_2$	285	31	29	89
	RuCoP	300	37	23	77
	Ni@Ni$_2$P–Ru HNRs	283	41	31	80
	Ru/MoS$_2$/CP	408	60	13	81
	NiRu@N–C	273	64	32	88
1.0 M PBS	Ru@Co–SAs/N–C	285	82	55	87
0.5 M H$_2$SO$_4$	PtRu@RFCS	354	27.2	19.7	74
	RuCoP	300	31	11	77
	v-Pt$_{29}$Pd$_3$Ru$_{62}$Te$_6$ AS	285	32	39	73
	Ni@Ni$_2$P–Ru HNRs	283	35		80
	NiRu@N–C	273	36	50	88
	CeO$_2$–Ru	197	41	47	83
	Ru–MoO$_2$	285	44	55	89
	Ru@Co–SAs/N–C	285	55	57	87
0.1 M HClO$_4$	h-PNROC		35	29.6	75

carbon shell on NiRu alloy nanoparticles formed during thermal annealing plays an important role in improving the HER activity and durability. For example, the carbon shell prevents corrosion and aggregation during long-term measurement, improves electron transfer, and provides sufficient localized reactive sites by modifying the charge distribution on the carbon layer. The as-prepared NiRu@N–C showed high HER catalytic performance with low Tafel slopes of 36 mV dec^{-1} in 0.5 M H$_2$SO$_4$ and 64 mV dec^{-1} in 1 M aq. KOH solution. Jiang *et al.*[89] designed a Ru–MoO$_2$ nanohybrid, because the strong electronic interaction between Ru and Mo would lead to boosting the electrical conductivity and efficiently reducing the energy barriers of intermediates.[56,90] Catalysts were prepared *via* a simple *in situ* thermal annealing of a Ru modified Mo-based MOF under an inert atmosphere. The nanocomposites exhibited low

overpotential at 10 mA cm^{-2} under both acidic (55 mV in 0.5 M aq. H$_2$SO$_4$) and alkaline (29 mV in 1 M aq. KOH) conditions, as the synergistic interplay induced strong electronic interactions between MoO$_2$ and Ru nanoparticles. They verified the origin of the improvement of the electrocatalytic performance using DFT calculations, XPS measurements, and electrochemical impedance spectra (EIS).

The HER performances of recently reported Ru catalysts on transition metals are summarized in Table 4.

6. Conclusion and perspectives

Recently, hydrogen energy from water splitting has been considered as clean and sustainable energy and as a possible

Table 5 Comparison of HER performances of precious metal containing composites

Reaction medium	Catalyst	Loading density ($\mu g\ cm^{-2}$)	Tafel slope ($mV\ dec^{-1}$)	Overpotential at 10 mA cm^{-2} (mV)	Ref.
0.5 M H$_2$SO$_4$	IrCo–PHNC*		26.6	21	91
	PtRu@RFCS	354	27.2	19.7	74
	Ru$_2$P/RGO	1000	29	22	59
	Au@PdAg NRBs		30	26.2	92
	Ru@GnP	750	30	13	27
	Ru@C$_2$N	285	30	13.5	12
	Ru/GLC	400	30	35	29
	Ru–NGC	360	31	25	45
	RuCoP	300	31	11	77
	Ru$_2$P/graphene	1000	32	18	58
	v-Pt$_{29}$Pd$_3$Ru$_{62}$Te$_6$ AS	285	32	39	73
0.1 M HClO$_4$	Pt/FeCo alloy/Cu/CNTs	280	24	18	93
1.0 M KOH	Ru-NC-700	200	14	12	42
	v-Pt$_{29}$Pd$_3$Ru$_{62}$Te$_6$ AS	285	22	20	73
	Ru@GnP	250	28	22	27
	Ir@CON	500	29	12.9	5
	Ru@Co–SAs/N–C	285	30	7	87
	Ru/NC		31	21	43
	RuCo@NC	275	31	28	78
	Ru-MoO$_2$	285	31	29	89

alternative to fossil fuels. To realize hydrogen economy, developing efficient and durable electrocatalysts for hydrogen evolution is one of the biggest challenges. To date, the champion catalysts for water splitting have been Pt-based ones. However, for widespread utilization, Pt has intrinsic problems coupled with its high cost, scarcity and instability. Thus, enormous efforts have been devoted to developing precious/non-precious metal and metal-free catalysts as alternatives to Pt-based catalysts. Very recently, there have been several reports on the outstanding HER performances of precious metal-based catalysts, such as iridium, platinum, gold, ruthenium, palladium, which are superior or competitive to the performance of commercial Pt/C (Table 5). Among those precious metal catalysts, this review is focused on the most promising Ru-based electrocatalysts, which have demonstrated outstanding HER activity in both acidic and alkaline electrolytes. More importantly, Ru is electrochemically durable and cost competitive compared to other precious metals. For a profound understanding, theoretical calculations of the binding energies of H, OH, and H_2O on the surface of Ru and Gibbs free energy are summarized along with experimental results.

To improve HER performance, various strategies have been adopted, such as boosting the electrical conductivity to facilitate electron transport using carbon materials, improving the electrocatalytic activity through incorporation of heteroatoms and/or transition metals, nanostructuring to increase the active sites, and reducing the content of Ru through MOF-assisted approaches and other unique strategies. Based on several studies related to Ru-based catalysts for the HER they have shown outstanding performance in all pH ranges. Specifically, under alkaline conditions, Ru-based catalysts have demonstrated even better performance than Pt/C due to their outstanding H_2O dissociation properties proved by their binding energies of OH and H_2O. In addition, the difference in electrocatalytic activity according to their crystal structures was also reported. However, the research results of Ru-based catalysts are very limited and their theoretical understanding is limited, because research studies in this field are still in their infant stages. Hence, there must be plenty of room for further improvements for one of the strongest prospects to realize hydrogen economy.

Future studies must be not only for improving the HER performance of Ru-based catalysts but also for fabricating water splitting devices in combination with electrodes for the oxygen evolution reaction (OER). In particular, additional fundamental understanding of the HER mechanisms is essential toward the design and synthesis of scalable, durable, and efficient catalysts at low-cost. In addition, it is absolutely necessary for the development of economically viable and safe water splitting devices. Such efforts may lead to the realization of hydrogen as a clean and sustainable energy source to replace fossil fuels.

Conflicts of interest

There are no conflicts to declare.

Acknowledgements

References

1 H. Fei, J. Dong, M. J. Arellano-Jiménez, G. Ye, N. Dong Kim, E. L. G. Samuel, Z. Peng, Z. Zhu, F. Qin, J. Bao, M. J. Yacaman, P. M. Ajayan, D. Chen and J. M. Tour, *Nat. Commun.*, 2015, **6**, 8668.

2 M. Zeng and Y. Li, *J. Mater. Chem. A*, 2015, **3**, 14942–14962.

3 Y. Liu, G. Yu, G.-D. Li, Y. Sun, T. Asefa, W. Chen and X. Zou, *Angew. Chem.*, 2015, **54**, 10752–10757.

4 M. Gong, W. Zhou, M.-C. Tsai, J. Zhou, M. Guan, M.-C. Lin, B. Zhang, Y. Hu, D.-Y. Wang, J. Yang, S. J. Pennycook, B.-J. Hwang and H. Dai, *Nat. Commun.*, 2014, **5**, 4695.

5 J. Mahmood, M. A. R. Anjum, S.-H. Shin, I. Ahmad, H.-J. Noh, S.-J. Kim, H. Y. Jeong, J. S. Lee and J.-B. Baek, *Adv. Mater.*, 2018, **30**, 1805606.

6 Y. Zheng, Y. Jiao, M. Jaroniec and S. Z. Qiao, *Angew. Chem.*, 2015, **54**, 52–65.

7 X. X. Zou and Y. Zhang, *Chem. Soc. Rev.*, 2015, **44**, 5148–5180.

8 Y. Zheng, Y. Jiao, Y. Zhu, L. H. Li, Y. Han, Y. Chen, A. Du, M. Jaroniec and S. Z. Qiao, *Nat. Commun.*, 2014, **5**, 3783.

9 Z.-F. Huang, J. Song, K. Li, M. Tahir, Y.-T. Wang, L. Pan, L. Wang, X. Zhang and J.-J. Zou, *J. Am. Chem. Soc.*, 2016, **138**, 1359–1365.

10 D. Strmcnik, P. P. Lopes, B. Genorio, V. R. Stamenkovic and N. M. Markovic, *Nano Energy*, 2016, **29**, 29–36.

11 Y. Zheng, Y. Jiao, Y. Zhu, L. H. Li, Y. Han, Y. Chen, M. Jaroniec and S.-Z. Qiao, *J. Am. Chem. Soc.*, 2016, **138**, 16174–16181.

12 J. Mahmood, F. Li, S.-M. Jung, M. S. Okyay, I. Ahmad, S.-J. Kim, N. Park, H. Y. Jeong and J.-B. Baek, *Nat. Nanotechnol.*, 2017, **12**, 441.

13 G. S. Karlberg, *Phys. Rev. B: Condens. Matter Mater. Phys.*, 2006, **74**, 153414.

14 T. R. Cook, D. K. Dogutan, S. Y. Reece, Y. Surendranath, T. S. Teets and D. G. Nocera, *Chem. Rev.*, 2010, **110**, 6474–6502.

15 M. Bajdich, M. García-Mota, A. Vojvodic, J. K. Nørskov and A. T. Bell, *J. Am. Chem. Soc.*, 2013, **135**, 13521–13530.

16 X. M. Li, X. G. Hao, A. Abudula and G. Q. Guan, *J. Mater. Chem. A*, 2016, **4**, 11973–12000.

17 X. Peng, C. Wei and W. Xin, *Adv. Energy Mater.*, 2015, **5**, 1500985.

18 J. Durst, A. Siebel, C. Simon, F. Hasché, J. Herranz and H. A. Gasteiger, *Energy Environ. Sci.*, 2014, **7**, 2255–2260.

19 S. Sultan, J. N. Tiwari, A. N. Singh, S. Zhumagali, M. Ha, C. W. Myung, P. Thangavel and K. S. Kim, *Adv. Energy Mater.*, 2019, **9**, 1900624.

20 D. V. Esposito, S. T. Hunt, Y. C. Kimmel and J. G. Chen, *J. Am. Chem. Soc.*, 2012, **134**, 3025–3033.

21 P. Liu and J. A. Rodriguez, *J. Am. Chem. Soc.*, 2005, **127**, 14871–14878.

22 R. R. Chianelli, G. Berhault, P. Raybaud, S. Kasztelan, J. Hafner and H. Toulhoat, *Appl. Catal., A*, 2002, **227**, 83–96.

23 G. Zhang, G. Wang, Y. Liu, H. Liu, J. Qu and J. Li, *J. Am. Chem. Soc.*, 2016, **138**, 14686–14693.

24 W. Sheng, M. Myint, J. G. Chen and Y. Yan, *Energy Environ. Sci.*, 2013, **6**, 1509–1512.

25 J. Greeley, T. F. Jaramillo, J. Bonde, I. Chorkendorff and J. K. Nørskov, *Materials for Sustainable Energy*, 2010, pp. 280–284.

26 S.-Y. Bae, I.-Y. Jeon, J. Mahmood and J.-B. Baek, *Chem. – Eur. J.*, 2018, **24**, 18158–18179.

27 F. Li, G.-F. Han, H.-J. Noh, I. Ahmad, I.-Y. Jeon and J.-B. Baek, *Adv. Mater.*, 2018, **30**, 1803676.

28 I.-Y. Jeon, Y.-R. Shin, G.-J. Sohn, H.-J. Choi, S.-Y. Bae, J. Mahmood, S.-M. Jung, J.-M. Seo, M.-J. Kim, D. Wook Chang, L. Dai and J.-B. Baek, *Proc. Natl. Acad. Sci. U. S. A.*, 2012, **109**, 5588–5593.

29 Z. Chen, J. Lu, Y. Ai, Y. Ji, T. Adschiri and L. Wan, *ACS Appl. Mater. Interfaces*, 2016, **8**, 35132–35137.

30 Q.-L. Zhu, W. Xia, T. Akita, R. Zou and Q. Xu, *Adv. Mater.*, 2016, **28**, 6391–6398.

31 L. Fan, P. F. Liu, X. Yan, L. Gu, Z. Z. Yang, H. G. Yang, S. Qiu and X. Yao, *Nat. Commun.*, 2016, **7**, 10667.

32 T. Qiu, Z. Liang, W. Guo, S. Gao, C. Qu, H. Tabassum, H. Zhang, B. Zhu, R. Zou and Y. Shao-Horn, *Nano Energy*, 2019, **58**, 1–10.

33 D. Yu, E. Nagelli, F. Du and L. Dai, *J. Phys. Chem. Lett.*, 2010, **1**, 2165–2173.

34 U. N. Maiti, W. J. Lee, J. M. Lee, Y. Oh, J. Y. Kim, J. E. Kim, J. Shim, T. H. Han and S. O. Kim, *Adv. Mater.*, 2014, **26**, 40–67.

35 K. N. Wood, R. O'Hayre and S. Pylypenko, *Energy Environ. Sci.*, 2014, **7**, 1212–1249.

36 Y. Li, L. A. Zhang, Y. Qin, F. Chu, Y. Kong, Y. Tao, Y. Li, Y. Bu, D. Ding and M. Liu, *ACS Catal.*, 2018, **8**, 5714–5720.

37 Z.-L. Wang, K. Sun, J. Henzie, X. Hao, C. Li, T. Takei, Y.-M. Kang and Y. Yamauchi, *Angew. Chem.*, 2018, **57**, 5848–5852.

38 J. Wang, Z. Wei, S. Mao, H. Li and Y. Wang, *Energy Environ. Sci.*, 2018, **11**, 800–806.

39 X. Liu, Y. Jiao, Y. Zheng, K. Davey and S.-Z. Qiao, *J. Mater. Chem. A*, 2019, **7**, 3648–3654.

40 J. K. Nørskov, T. Bligaard, J. Rossmeisl and C. H. Christensen, *Nat. Chem.*, 2009, **1**, 37.

41 K. Kusada, H. Kobayashi, T. Yamamoto, S. Matsumura, N. Sumi, K. Sato, K. Nagaoka, Y. Kubota and H. Kitagawa, *J. Am. Chem. Soc.*, 2013, **135**, 5493–5496.

42 B. Lu, L. Guo, F. Wu, Y. Peng, J. E. Lu, T. J. Smart, N. Wang, Y. Z. Finfrock, D. Morris, P. Zhang, N. Li, P. Gao, Y. Ping and S. Chen, *Nat. Commun.*, 2019, **10**, 631.

43 J. Zhang, P. Liu, G. Wang, P. P. Zhang, X. D. Zhuang, M. W. Chen, I. M. Weidinger and X. L. Feng, *J. Mater. Chem. A*, 2017, **5**, 25314–25318.

44 K. Shen, X. Chen, J. Chen and Y. Li, *ACS Catal.*, 2016, **6**, 5887–5903.

45 Q. Song, X. Qiao, L. Liu, Z. Xue, C. Huang and T. Wang, *Chem. Commun.*, 2019, **55**, 965–968.

46 G. Ćirić-Marjanović, *Synth. Met.*, 2013, **177**, 1–47.

47 J. Tian, Q. Liu, N. Cheng, A. M. Asiri and X. Sun, *Angew. Chem.*, 2014, **53**, 9577–9581.

48 Z. Huang, Z. Chen, Z. Chen, C. Lv, H. Meng and C. Zhang, *ACS Nano*, 2014, **8**, 8121–8129.

49 P. Xiao, M. A. Sk, L. Thia, X. Ge, R. J. Lim, J.-Y. Wang, K. H. Lim and X. Wang, *Energy Environ. Sci.*, 2014, **7**, 2624–2629.

50 C. Y. Son, I. H. Kwak, Y. R. Lim and J. Park, *Chem. Commun.*, 2016, **52**, 2819–2822.

51 E. J. Popczun, C. G. Read, C. W. Roske, N. S. Lewis and R. E. Schaak, *Angew. Chem.*, 2014, **53**, 5427–5430.

52 E. J. Popczun, J. R. McKone, C. G. Read, A. J. Biacchi, A. M. Wiltrout, N. S. Lewis and R. E. Schaak, *J. Am. Chem. Soc.*, 2013, **135**, 9267–9270.

53 J. Gopalakrishnan, S. Pandey and K. K. Rangan, *Chem. Mater.*, 1997, **9**, 2113–2116.

54 Y. Kanda, C. Temma, K. Nakata, T. Kobayashi, M. Sugioka and Y. Uemichi, *Appl. Catal., A*, 2010, **386**, 171–178.

55 C. M. Lukehart, S. B. Milne and S. R. Stock, *Chem. Mater.*, 1998, **10**, 903–908.

56 Q. Li, Z.-L. Wang, G.-R. Li, R. Guo, L.-X. Ding and Y.-X. Tong, *Nano Lett.*, 2012, **12**, 3803–3807.

57 S. Carenco, D. Portehault, C. Boissière, N. Mézailles and C. Sanchez, *Chem. Rev.*, 2013, **113**, 7981–8065.

58 T. Liu, J. Wang, C. Zhong, S. Lu, W. Yang, J. Liu, W. Hu and C. M. Li, *Chem. – Eur. J.*, 2019, **25**, 7826–7830.

59 T. Liu, S. Wang, Q. Zhang, L. Chen, W. Hu and C. M. Li, *Chem. Commun.*, 2018, **54**, 3343–3346.

60 N. Danilovic, R. Subbaraman, D. Strmcnik, K.-C. Chang, A. P. Paulikas, V. R. Stamenkovic and N. M. Markovic, *Angew. Chem.*, 2012, **51**, 12495–12498.

61 Z. Pu, I. S. Amiinu, Z. Kou, W. Li and S. Mu, *Angew. Chem.*, 2017, **129**, 11717–11722.

62 Z. Shi, K. Nie, Z.-J. Shao, B. Gao, H. Lin, H. Zhang, B. Liu, Y. Wang, Y. Zhang, X. Sun, X.-M. Cao, P. Hu, Q. Gao and Y. Tang, *Energy Environ. Sci.*, 2017, **10**, 1262–1271.

63 H. Ang, H. T. Tan, Z. M. Luo, Y. Zhang, Y. Y. Guo, G. Guo, H. Zhang and Q. Yan, *Small*, 2015, **11**, 6278–6284.

64 J.-Q. Chi, W.-K. Gao, J.-H. Lin, B. Dong, K.-L. Yan, J.-F. Qin, B. Liu, Y.-M. Chai and C.-G. Liu, *ChemSusChem*, 2018, **11**, 743–752.

65 J. Yang, B. Chen, X. Liu, W. Liu, Z. Li, J. Dong, W. Chen, W. Yan, T. Yao, X. Duan, Y. Wu and Y. Li, *Angew. Chem.*, 2018, **57**, 9495–9500.

66 T. M. Tolhurst, C. Braun, T. D. Boyko, W. Schnick and A. Moewes, *Chem. – Eur. J.*, 2016, **22**, 10475–10483.

67 Q. Chang, J. Ma, Y. Zhu, Z. Li, D. Xu, X. Duan, W. Peng, Y. Li, G. Zhang, F. Zhang and X. Fan, *ACS Sustainable Chem. Eng.*, 2018, **6**, 6388–6394.

68 Y. Yang, Z. Lun, G. Xia, F. Zheng, M. He and Q. Chen, *Energy Environ. Sci.*, 2015, **8**, 3563–3571.

69 J. R. Kitchin, J. K. Nørskov, M. A. Barteau and J. G. Chen, *Phys. Rev. Lett.*, 2004, **93**, 156801.

70 C. Chen, Y. Kang, Z. Huo, Z. Zhu, W. Huang, H. L. Xin, J. D. Snyder, D. Li, J. A. Herron, M. Mavrikakis, M. Chi, K. L. More, Y. Li, N. M. Markovic, G. A. Somorjai, P. Yang and V. R. Stamenkovic, *Science*, 2014, **343**, 1339–1343.

71 H. Ma, P. Chen, B. Li, J. Li, R. Ai, Z. Zhang, G. Sun, K. Yao, Z. Lin, B. Zhao, R. Wu, X. Tang, X. Duan and X. Duan, *Nano Lett.*, 2018, **18**, 3523–3529.

72 Y. Wang, Y. Li and T. Heine, *J. Am. Chem. Soc.*, 2018, **140**, 12732–12735.

73 S. Liu, X. Mu, W. Li, M. Lv, B. Chen, C. Chen and S. Mu, *Nano Energy*, 2019, **61**, 346–351.

74 K. Li, Y. Li, Y. Wang, J. Ge, C. Liu and W. Xing, *Energy Environ. Sci.*, 2018, **11**, 1232–1239.

75 A. Oh, H. Y. Kim, H. Baik, B. Kim, N. K. Chaudhari, S. H. Joo and K. Lee, *Adv. Mater.*, 2019, **31**, 1805546.

76 N. Du, C. Wang, X. Wang, Y. Lin, J. Jiang and Y. Xiong, *Adv. Mater.*, 2016, **28**, 2077–2084.

77 J. Xu, T. Liu, J. Li, B. Li, Y. Liu, B. Zhang, D. Xiong, I. Amorim, W. Li and L. Liu, *Energy Environ. Sci.*, 2018, **11**, 1819–1827.

78 J. Su, Y. Yang, G. Xia, J. Chen, P. Jiang and Q. Chen, *Nat. Commun.*, 2017, **8**, 14969.

79 J. Deng, P. Ren, D. Deng and X. Bao, *Angew. Chem.*, 2015, **54**, 2100–2104.

80 Y. Liu, S. Liu, Y. Wang, Q. Zhang, L. Gu, S. Zhao, D. Xu, Y. Li, J. Bao and Z. Dai, *J. Am. Chem. Soc.*, 2018, **140**, 2731–2734.

81 J. Liu, Y. Zheng, D. Zhu, A. Vasileff, T. Ling and S.-Z. Qiao, *Nanoscale*, 2017, **9**, 16616–16621.

82 B. Hinnemann, P. G. Moses, J. Bonde, K. P. Jørgensen, J. H. Nielsen, S. Horch, I. Chorkendorff and J. K. Nørskov, *J. Am. Chem. Soc.*, 2005, **127**, 5308–5309.

83 E. Demir, S. Akbayrak, A. M. Önal and S. Özkar, *ACS Appl. Mater. Interfaces*, 2018, **10**, 6299–6308.

84 A. Trovarelli and J. Llorca, *ACS Catal.*, 2017, **7**, 4716–4735.

85 H. Furukawa, K. E. Cordova, M. O'Keeffe and O. M. Yaghi, *Science*, 2013, **341**, 1230444.

86 N. Stock and S. Biswas, *Chem. Rev.*, 2012, **112**, 933–969.

87 S. Yuan, Z. Pu, H. Zhou, J. Yu, I. S. Amiinu, J. Zhu, Q. Liang, J. Yang, D. He, Z. Hu, G. Van Tendeloo and S. Mu, *Nano Energy*, 2019, **59**, 472–480.

88 Y. Xu, S. Yin, C. Li, K. Deng, H. Xue, X. Li, H. Wang and L. Wang, *J. Mater. Chem. A*, 2018, **6**, 1376–1381.

89 P. Jiang, Y. Yang, R. Shi, G. Xia, J. Chen, J. Su and Q. Chen, *J. Mater. Chem. A*, 2017, **5**, 5475–5485.

90 C. G. Morales-Guio, L.-A. Stern and X. Hu, *Chem. Soc. Rev.*, 2014, **43**, 6555–6569.

91 J. Feng, F. Lv, W. Zhang, P. Li, K. Wang, C. Yang, B. Wang, Y. Yang, J. Zhou, F. Lin, G.-C. Wang and S. Guo, *Adv. Mater.*, 2017, **29**, 1703798.

92 Z. Fan, Z. Luo, X. Huang, B. Li, Y. Chen, J. Wang, Y. Hu and H. Zhang, *J. Am. Chem. Soc.*, 2016, **138**, 1414–1419.

93 J. N. Tiwari, S. Sultan, C. W. Myung, T. Yoon, N. Li, M. Ha, A. M. Harzandi, H. J. Park, D. Y. Kim, S. S. Chandrasekaran, W. G. Lee, V. Vij, H. Kang, T. J. Shin, H. S. Shin, G. Lee, Z. Lee and K. S. Kim, *Nat. Energy*, 2018, **3**, 773–782.